LAWRENCE
LIVERMORE
NATIONAL
LABORATORY

LLNL-JRNL-679896

Light Self-focusing in the Atmosphere: Thin Window Model

I. A Vaseva, M. P. Fedoruk, A. M. Rubenchik, S. K. Turitsyn

December 3, 2015

Scientific Reports

Disclaimer

This document was prepared as an account of work sponsored by an agency of the United States government. Neither the United States government nor Lawrence Livermore National Security, LLC, nor any of their employees makes any warranty, expressed or implied, or assumes any legal liability or responsibility for the accuracy, completeness, or usefulness of any information, apparatus, product, or process disclosed, or represents that its use would not infringe privately owned rights. Reference herein to any specific commercial product, process, or service by trade name, trademark, manufacturer, or otherwise does not necessarily constitute or imply its endorsement, recommendation, or favoring by the United States government or Lawrence Livermore National Security, LLC. The views and opinions of authors expressed herein do not necessarily state or reflect those of the United States government or Lawrence Livermore National Security, LLC, and shall not be used for advertising or product endorsement purposes.

Light Self-focusing in the Atmosphere: Thin Window Model

Irina A. Vaseva [1,2], Mikhail P. Fedoruk [1,2], Alexander M. Rubenchik [3], Sergei K. Turitsyn [1,4]

[1]Novosibirsk State University, 2 Pirogova Street, Novosibirsk, 630090, Russia

[2]Institute of Computational Technologies, Siberian Branch of the Russian Academy of Sciences, 6 Ac. Lavrentjev Avenue, Novosibirsk

[3]Lawrence Livermore National Laboratory, Livermore, California 94550, USA

[4]Aston Institute of Photonic Technologies, School of Engineering and Applied Science, Aston University, Birmingham, B4 7ET, UK

Correspondence: Prof. S. K. Turitsyn, Aston Institute of Photonic Technologies, School of Engineering and Applied Science, Aston University, Birmingham B4 7ET, UK; Tel. + 44 121 204 3538
Fax: + 44 121 204 3682; E-mail: s.k.turitsyn@aston.ac.uk

Abstract
Ultra-high power (exceeding the self-focusing threshold by more than three orders of magnitude) light beams from ground-based laser systems may find applications in space-debris cleaning. The propagation of such powerful laser beams through the atmosphere reveals many novel and interesting features compared to traditional light self-focusing. We demonstrate here that for the relevant laser parameters, when the thickness of the atmosphere is much shorter than the focusing length (that is, of the orbit scale), the beam transit through the atmosphere in lowest order produces phase distortion only. This means that by using adaptive optics it may be possible to eliminate completely the impact on the laser beam of self-focusing effects in the atmosphere. The area of applicability of the proposed "thin window" model is broader than the specific physical problem considered here. For instance, it might find applications in femtosecond laser materials processing.

Keywords: laser, self-focusing, space debris

Introduction

A ground-based pulsed laser system is a promising way to mitigate the growing space debris problem [1]. Following decades of space exploration, an ever-growing cloud of more than twenty-two thousand pieces of space debris is now orbiting the Earth, posing a serious treat to satellites and corresponding technologies and services. A debris-removal laser system with an ultra-long reach (on the scale of the distance to the orbit) must exploit ultra-high power beams with a power exceeding the self-focusing threshold by more than three orders of magnitude. The propagation of a pre-focused (spatial pre-chirping) high-power laser beam through the atmosphere is very different from studies of conventional self-focusing and filamentation in air or gases. The important new feature is that such a pre-focused beam may be free of filamentation even for very high input power [1, 2]. Recently it was demonstrated that for the typical parameters of a laser pulse, self-focusing in the atmosphere can impair the laser beam quality, decreasing the laser intensity on the debris and degrading the system performance [2]. To some extent, the effect of the self-focusing can be compensated by pre-defocusing of the initial beam. However, the optimization of the pre-focusing requires complex and time-consuming modeling.

LLNL-JRNL-679896

Here we demonstrate that the situation can be accurately modeled within the "thin window" (TW) approximation [3]. When the thickness of the atmosphere is much smaller than the focusing length, propagation through the atmosphere results in phase distortion only. Due to the exponential decay of the nonlinear effects, the remaining propagation (beyond the atmosphere) is effectively linear, greatly simplifying modeling. Effectively this can be treated as split-step approach with just one nonlinear step and one linear step to model beam propagation. We show here that the TW model prediction is in excellent agreement with solutions of the exact nonlinear Schrödinger equation (NLSE). Using the TW model we are able to calculate the optimal focusing conditions to compensate maximally the aberration produced by self-focusing in the atmosphere. We have also calculated the reduction in the peak intensity at the focal plane due to the non-compensated aberrations and the displacement of the focal point.

The high accuracy of the TW model has an important practical application. Using adaptive optics one can apply an initial phase pre-distortion, which compensates the nonlinear phase changes. We will demonstrate that as a result one can have an almost perfect Gaussian beam at the atmospheric exit, and the detrimental effects of self-focusing can be eliminated to a great extent.

For most of the applications considered here, it is sufficient to know only the intensity in the spot center and the spot size [1] (effectively, it suffices to know just the ratio of these values for an aberrated beam compared to the ideal Gaussian one). We present simple analytical expressions for these important practical parameters based on the TW model and verify their applicability through numerical modeling using the NLSE.

The operation of the complex laser system considered here depends on numerous parameters, such as pulse energy, focusing mirror size, focal distance, laser system altitude, and others. As a result, the direct system optimization, although possible, requires much time-consuming effort. Our model indicates that there exists a scaling in the problem, determined by a combination of the key parameters. This scaling makes it possible to relate the results for different sets of parameters and greatly reduces the optimization efforts.

Materials and Methods

Thin Window (TW) model

The analysis of the ground-based laser system for space debris cleaning indicates that the laser power must greatly exceed, by a factor of 1000-5000, the critical power P_{cr} for self-focusing in the atmosphere [2, 4]. The self-focusing length in this situation is much longer than the atmospheric thickness, and nonlinear effects produce only phase aberrations, which during the ensuing long (about 1000 km) free propagation to the debris can greatly modify the beam (see Fig. 1). One can see that as a result of the nonlinear focusing in the atmosphere, the intensity peak moves back to the ground, and at high power when filamentation becomes important, the transverse beam shape is far from Gaussian. Let us consider the problem in more detail.

The propagation of the laser beam is described by the nonlinear Schrodinger equation [2, 4], i.e.

$$i\frac{\partial \Psi}{\partial z'} + \frac{1}{2n_0 k_0}\Delta_\perp \Psi + k_0 n_2(z')\,|\,\Psi\,|^2\ \Psi = 0$$

where $\Delta_\perp$ is the two-dimensional Laplacian operator. The analysis in [4] demonstrates that the optimal pulse length, based on physics and engineering considerations, is on the order of a few nanoseconds. For this order of pulse length, temporal dispersion can be neglected in the main order of the considered effects. The inhomogeneity of the density must be taken into account in the nonlinearity only [1, 2, 4].

Here we consider a laser beam propagating vertically (relative to the ground). This is not very different from the optimal angle for the interaction with debris, which is about 30 degrees from the vertical [4]. The assumption of perpendicular propagation is not critically important, but it simplifies the presentation. It is customary to introduce dimensionless variables via:

$$\Psi(z',\vec{r}') = \sqrt{\frac{P_0}{R_0^2}} A(z,\vec{r}),$$

where $z = z'/L_D$ and $r = r'/R_0$. Here we have taken:

$L_D = 2n_0 k_0 R_0^2 = 4\pi\, n_0\, R_0^2 / \lambda_0$, $\quad k_0 = 2\pi/\lambda_0$, $\quad \lambda_0 = 1.06\ \mu\text{m}$, $\quad k_0 = 5.93\ \mu\text{m}^{-1}$, $\quad n_0 = 1.0$, $n_2(0) = 4.2\times 10^{-19}\ \text{cm}^2/\text{W}$,

with $z = 0$ corresponding to sea level. We assume the commonly used exponential density dependence with the atmosphere height $Z_0 = 6\text{km}$, $n(z')/n(0) = \exp(-z'/Z_0)$. The nonlinear effects decay with height as $n_2(z') = n_2(0)\cdot\exp(-z'/Z_0)$ [1,2]. Here a normalization parameter R_0 corresponds to the initial radius of the beam. The power is normalized by the value $P_0 = \lambda_0^2/(8\pi^2 n_0 n_2(0))$. The debris is located at the distance L. The resulting normalized equation has the form:

$$i\frac{\partial A}{\partial z} = -\Delta_\perp A - \exp(-z/h)\,|A|^2\, A, \qquad (1)$$

where $h = Z_0/L_D$. For $R_0 = 1\text{m}$ and the parameters given above, we have $L_D = 11855\ \text{km}$, $P_0 = 0.339\text{GW}$ and $P_{cr} = 4\pi P_0 = 4.258\ \text{GW}$ for a Gaussian input beam.

It is possible to show that the fastest growing perturbations resulting in filamentation are axisymmetric [5], and that filamentation, at least initially, breaks the beam into ring-like structures. The formation and break-up of the ring structure is the well-documented pathway to Gaussian beam filamentation [6], and beam propagation can be described in the main order within the axisymmetric version of Eq. (1).

The problem is characterized by three dimensionless parameters: the ratio P_{in}/P_{cr} of the input beam power P_{in} to the critical power, the initial beam pre-focusing parameter C (see below), and a parameter h characterizing decay of the nonlinear effects with distance, typically $h \ll 1$. Let us consider the propagation of an initially Gaussian laser beam. On the surface at $z = 0$:

$$A(r, z=0) = \sqrt{\frac{P_{in}}{\pi}}\exp[-\frac{(1+iC)\,r^2}{2}] = \sqrt{I_0}\exp[-\frac{(1+iC)\,r^2}{2}]\cdot \qquad (1a)$$

Here P_{in} is the normalized input power of the laser beam, the dimensionless parameter $C = k_0\cdot R_0^2/F = L_D/2F$ is the initial beam pre-focusing parameter, and $I_0 = I(0,0) = P_{in}[W]/(\pi P_0[W]) = 4P_{in}/P_{cr}$. F has the meaning of a focal distance that in this case is a debris height L. Therefore, the dimensional initial pre-focusing is given by $C = L_D/2L$

We would like to stress that the problem under consideration, though similar in terms of the basic equations to numerous self-focusing studies (see e.g. [3, 7] and references therein), is rather different in terms of underlying physics. The nonlinearity decays exponentially with propagation. Therefore, the system is strongly inhomogeneous with spatially decreasing nonlinear effects. Our laser beam has a much larger spot size (over 1m). The self-focusing length $L_{SF} \propto L_D / \sqrt{P_{in} / P_{cr} - 1}$ is much longer than the thickness of the atmosphere. This displaces the self-focusing (beam collapse) point far beyond the atmosphere. In other words, we consider here light propagation over a finite distance (the thickness of the nonlinear layer), with the focusing point located beyond this region, where the propagation is linear. In this case the self-focusing effect compresses the beam, but without the catastrophic collapse of all the energy into a small volume. Numerical modeling [2] strongly indicates that for the problem examined here, even for input powers well above the critical power for self-focusing, the beam can maintain its integrity and is focused as a whole.

Let us now apply in this context the thin window model, following [3,7-9]. We replace the numerical calculation of the propagation described by Eq. (1) by just one an effective nonlinear step and ensuing linear propagation. After propagation of the short distance z_1 the impact of the nonlinear term in Eq. (1) can be formally written as:

$$A(r, z_1) = \exp\left[i \int_0^{z_1} \eta(z) |A(r, 0)|^2 \, dz \right] A(r,0) \qquad (2)$$

When the beam propagates up to atmospheric boundaries, the impact of the diffraction can be estimated as $\sim z_1 \sim h \sim Z_0 / L_D \sim 10^{-3} << 1$, and the effect of the nonlinearity can be estimated as hP_{in} / P_{cr}, which can be larger than unity. As the nonlinearity is decaying exponentially, the initial propagation stage is the most important and after it, propagation is linear with a modified phase. Our approach is based on the observation that during propagation through the atmosphere, with high accuracy we can disregard the mutual impact of the nonlinearity and diffraction. Taking into account only the phase distortion due to nonlinearity, the laser field after propagation through the atmosphere is given by Eq. (2).

For a Gaussian initial beam we have the explicit description of the field:

$$A(r, z_1) = \sqrt{I_0} \exp[-\frac{r^2}{2} - i(\frac{Cr^2}{2} - \Phi)], \qquad (3)$$

where $\Phi = b \times \exp(-r^2)$, $b = I_0 h [1 - \exp(-z_1 / h)]$, $I_0 = I(0,0) = P_{in}[W] / (\pi P_0[W]) = 4P_{in} / P_{cr}$. The parameter b has the meaning of the nonlinear phase shift scale. As we will show below, it is important for understanding the ensuing linear dynamics.

The value of z_1 that is certainly a critical parameter of the model is approximately several times h; the optimal choice of z_1 will be further discussed below, after comparison with numerical modeling results. It is clear that there must exist an optimal value of z_1, since for small z_1 we cut out the part of the atmospheric propagation, and when z_1 is too large the free propagation will modify the solution (the window is no longer thin). Due to the exponential dependence on z_1 in (3), the optimal value is about a few atmospheric thicknesses. Let us make some estimates. We require the maximal phase deviation at $z = z_1$ to be different from that at infinite z by less than α radians. In this case, z_1 is given by $z_1 / h = \ln(I_0 h / \alpha)$. Due to the logarithmic dependence, z_1 depends only weakly on the laser power and the choice of α. For α = 0.01, z_1 in dimensional units increases from 36 km to 45 km when the power changes

from P = 1000 P_{cr} to 5000 P_{cr}, and the choice of z_1 does not strongly affect the results. The following results will be presented for some particular z_1 values, and the impact of the choice of z_1 on the results obtained by the TW model will be discussed in detail in Appendix I below.

After the beam exits the atmosphere, it undergoes almost free linear propagation (see Fig. 2). From Eq. (3) we see that the phase is not quadratic, and the ensuing beam propagation is not described by the simple formula available for the focused Gaussian input. The curvature of the phase corresponds to an additional focusing, and the atmosphere serves as a focusing astigmatic lens. As a result, the maximal field intensity is reached before the linear focal plane. By varying the pre-focusing parameter C (or even adjusting the initial beam phase to compensate more accurately for the nonlinear phase aberration using adaptive optics) we can partially compensate for the propagation through the atmosphere [2].

To evaluate the field in the focal plane, consider the solution of the linear problem [Eq. (1) without nonlinear term]:

$$i\frac{\partial A}{\partial z} = -\Delta_{\perp} A \qquad (4)$$

The solution of Eq. (4) at a distance z can be expressed using a well-known Green's function in terms of the field at $z = z_0$, $A(x, y, z = z_0) = A_1(x, y)$, namely:

$$A(x, y, z) = -i\frac{1}{4\pi(z - z_0)}\int dx_1 dy_1 A_1(x_1, y_1)\exp[i\frac{(x - x_1)^2 + (y - y_1)^2}{4(z - z_0)}] \qquad (5)$$

Assuming that the beam at $z = z_0$ to satisfies Eq. (3), we can write down explicitly the focusing part:

$$A(x, y, z = z_0) = U(x, y)\exp[-i\frac{r^2}{4L}] \qquad (6)$$

where $r^2 = x^2 + y^2$ and $U(x, y) = \exp[-\frac{r^2}{2} - i\Phi]$. Substitution of this expression into Eq. (5) yields

$$A(x, y, z) = -i\frac{\exp[i\frac{r^2}{4(z - z_0)}]}{4\pi(z - z_0)}\int dx_1 dy_1 U(x_1, y_1)\exp[-i\frac{(xx_1 + yy_1)}{2(z - z_0)}]\exp[i\frac{x_1^2 + y_1^2}{4}(\frac{1}{z - z_0} - \frac{1}{L})] \qquad (7)$$

We see that at the focal plane z = z_0+L, the Fresnel quadratic terms are cancelled and the electric field is proportional to the Fourier transform of the field on the boundary [4].

$$A(x, y, L) = -i\frac{\exp[i\frac{r^2}{4L}]}{4\pi L}\int dx_1 dy_1 U(x_1, y_1)\exp[-i\frac{xx_1 + yy_1}{2L}] = -i\frac{\exp[i\frac{r^2}{4L}]}{4\pi L}U_q; \vec{q} = \frac{\vec{r}}{2L} \qquad (8)$$

We focus in what follows only on the axisymmetric beam propagation. The general solution of the linear problem (5) for the axisymmetric case can be transformed to the form:

$$A(r,z) = -\frac{i}{2(z-z_0)}\int_0^\infty ds\, s\, R(s)\, J_0[\frac{s\, r}{2(z-z_0)}]\times \exp[i\,\frac{(s^2+r^2)}{4(z-z_0)}]$$

where $R(r) = A(r, z = z_0)$. Applying the explicit extraction of the focusing factor $R(s) = U(s)\exp[-\frac{is^2}{4L}]$, we see that again in the focal plane z = z_0+L the Fresnel terms are cancelled and the electric field at the focal plane is proportional to the Fourier transform of the field at the boundary. To keep a focal point at the same distance z = L, we can either account for the effective linear phase change during the propagation from z = 0 to z = z_1 or consider linear propagation from z = 0 with a phase modified due to nonlinear effects – an effective split step method with just one nonlinear and one linear steps. Here, for simplicity, we use the latter (use $z_0 = 0$) and demonstrate excellent agreement between this simplified TW approach and the full numerical modelling of the NLS equation.

As a matter of fact, in practical applications, one usually needs only a subset of this full field description, namely, information about the intensity on the target. Specifically, one needs the intensity in the spot center and the average spot size. Therefore, the description can be further simplified.

Assuming that the field at $z = z_0$ is $A(r, z_0) = U(r)\exp[-\frac{ir^2}{4L}]$, the electric field on the target in the focal plane can be presented as a Fourier transform of that in Eq. (8) [10]. Specifically, the field in the spot center is given by the expression:

$$A(0,0,z=L) = -\frac{i}{4L}\int U(x_1,y_1)dx_1dy_1 = -\frac{i\pi}{2L}\int U(r)rdr$$

It is customary to use the Strehl ratio S, the ratio of the intensity in the center to that produced by the linear evolution of the Gaussian beam (1a):

$$S = \frac{\left|\int U(r)rdr\right|^2}{\left|\int U_G(r)rdr\right|^2}, \qquad (9)$$

Recalling that $U(r) = \sqrt{I_0}\exp[-\frac{r^2}{2} + i\Phi]$, $U_G(r) = \sqrt{I_0}\exp[-\frac{r^2}{2}]$, we can calculate the Strehl ratio explicitly:

$$S = \left|\int_0^1 \exp[ibx^2]dx\right|^2 = \frac{\pi}{2b}\left|C(\sqrt{\frac{2b}{\pi}}) + iS(\sqrt{\frac{2b}{\pi}})]\right|^2 = \frac{\pi}{4b}\left|erf[(1-i)\sqrt{\frac{b}{2}}]\right|^2 \qquad (9a)$$

The integral estimate of the square of the spot size on the target can be calculated in a similar way as follows:

$$\pi\langle r^2\rangle = \frac{\int r^2\left|A(r,L)\right|^2 rdr}{\int \left|A(r,L)\right|^2 rdr} = \frac{4L^2\int\left|\frac{\partial U}{\partial r}\right|^2 rdr}{\int\left|U\right|^2 rdr} \qquad (10)$$

Similarly, it is convenient to calculate analytically the beam quality parameter M^2, the ratio spot size squared (9) to the value calculated for the Gaussian beam:

$$M^2 = \frac{\int r^2 |A(r,L)|^2 rdr}{\int r^2 |A_G(r,L)|^2 rdr} = \frac{\int \left|\frac{\partial U(r)}{\partial r}\right|^2 rdr}{\int \left|\frac{\partial U_G(r)}{\partial r}\right|^2 rdr} = 1 + \frac{4b^2}{9} \qquad (11)$$

Results and Discussion

Comparison with the direct numerical modelling

Figures 3-7 demonstrate that the results obtained by using the simple TW model are in good agreement with the direct NLSE simulations. In Fig. 3 we present the peak intensity distribution along z for the TW model of Eq. (3) and the corresponding NLSE solution. Here h = 0.000506, $C = k_0 R_0^2 / L$ =5.93, L = 1000 km, R_0 = 1 m, λ_0 = 1.06 μm and P_{in}/P_{cr} = 1500 and 5000, with the corresponding factor nonlinear phase shift b = 3.02 or b = 10.05, respectively. Here and below (unless other values are mentioned specifically), the parameter z_1 in the TW model is 30 km. In the numerical modelling we use (3) as the boundary condition for the linear propagation starting at z_0= 0.

Figure 3 shows an excellent agreement between the TW model and the full numerical simulations based on the NLS equation, both for evolution of the peak intensity with distance and for the radial beam intensity distribution. One can see that the TW model approximates well the exact solution of the NLSE even in the situation with well-developed filamentation (see Fig. 1b), with the field distribution being very far from the Gaussian beam. Note that in the TW model the solution depends on the dimensionless parameter $b = I_0 h[1 - \exp(-z_1 / h)]$ only, which simplifies the system optimization.

Let us discuss the calculations of the Strehl ratio. For the TW model (3), S can be calculated analytically [Eq. (9a)]. The results are not sensitive to the value of z_1 The comparison of the Strehl ratio computed with the NLSE solution (1) and the TW model (9a) is plotted in Fig. 4(a). We see that the TW model is very close to the NLSE solution, reproducing even non-monotonic S behavior. Let us stress again that the TW model is accurate for the calculation of intensity in spot center even at large b, when the beam is far from Gaussian.

The calculations of beam quality (M^2) are presented in Fig. 4 (b). Within the TW model Eq. (3), M^2 can be calculated analytically [Eq. (11)]. It is important to note that this result is valid for beams quite different from Gaussian. We see that the TW model provides an excellent description at modest b and slightly overestimates beam quality for large b, when the beam is already destroyed.

As we discussed above, the detrimental effects of self-focusing can be partially compensated by additional defocusing the beam by the quadratic (in radius) phase pre-distortion with the modified chirp. Mathematically, this means that instead of the previous chirp parameter C we use the modified $C_{opt.}$ Analytically, the optimal focusing parameter C_{opt} is a function of b. The optimal chirp gives the maximum

intensity at the destination point L = 1000 km. The graph of the optimal C_{opt} as a function of b is presented in Fig. 5 (a). Here $C = k_0R_0^2/L = 5.93$, corresponding to a focal point L. The peak intensity at the initial focal point L corresponding to the initial chirp C and optimal chirp C_{opt} is presented in Fig. 5 (b). Figure 5 (c) demonstrates that the TW model gives very accurate predictions for the shifted focal points F. Self-focusing changes the peak intensity, with the result depending on b as shown in Fig. 5 (d). We see that the initial defocusing can noticeably increase the Strehl ratio (see Fig. 5 (b)), and that the TW model is good for predicting the optimal focusing parameters.

Compensation of atmospheric aberrations by adaptive optics

The initial phase pre-distortion can be used to compensate the nonlinear phase changes. As a result, one can have an almost perfect Gaussian beam at the atmospheric exit, and detrimental effects of self-focusing can be eliminated to a great extent. The new initial condition with corrected phase are:

$$A(r,0) = \sqrt{I_0}\exp[-\frac{r^2}{2} - i(\frac{Cr^2}{2} + \Phi)], \qquad (13)$$

where $\Phi = b\exp(-r^2),\ b = I_0 h[1-\exp(-z_1/h)],\ I_0 = I(0,0) = 4P/P_{cr}$. Here z_1 = 30 km.

We compare the solution of the NLSE (1) with the initial condition (1a) and chirp C = 5.93 which corresponds to linear focusing at L = 1000 km; the solution of the same problem with optimal chirp $C_{opt} = 0.81C_0$; and the solution of the NLSE (1) with a pre-imposed phase, phase (13); and the solution of the linear problem (4) with initial condition (1a). The result is presented in Fig. 6. We see that the initial phase modification compensates nonlinear effects, and the solution of the NLSE is very close to the linear one. Note that, as expected, the solution of the NLSE with pre-imposed phase correction (13) preserves the Gaussian shape in the transverse directions.

We have demonstrated that the nonlinear effect of self-focusing in the atmosphere for space debris cleaning can be described with good accuracy within the thin window model. Within this model, the nonlinearity produces phase front distortion, serving as a high aberration focusing lens. Optical phase distortion results in displacement of the focusing point and beam filamentation, degrading the system performance. The former effect can be compensated partially by defocusing the initial beam. The TW model yields semi-analytical expressions for the calculation of peak intensity on debris (Strehl number) and beam quality M^2.

Typically, the nonlinear evolution of self-focusing can be approximated as a fixed shape beam propagation with slowly varying parameters. The equations for these parameters can be derived from the Talanov virial theorem or from the a variational principle [11,12]. Attempts to use this approach for the specific problem considered above failed due to beam filamentation and destruction. On the other hand, the TW model describes beam focusing with strong aberrations, with field distributions in the focal plane far from Gaussian. The pattern of the laser field is determined by a single dimensionless parameter b, similar to the B integral used in laser design to control the self-phase modulation. The dependence on only one parameter greatly simplifies the optimization of the beam pre-focusing arrangements.

The description of linear propagation after exit from the atmosphere can be simplified using the fact that the field in the focal plane is proportional to the Fourier transform of the field exiting the atmosphere. As

a result, we obtained simple expressions for the peak intensity (Strehl ratio) and beam quality M^2 which can be calculated in term of the exiting field.

Because of the high accuracy of the TW model, one can compensate for self-focusing in the atmosphere by a pre-imposed phase distribution which will cancel the nonlinear phase acquired during propagation in the atmosphere. Our modeling demonstrates that the detrimental effects off self-focusing can be almost completely eliminated by a pre-imposed phase calculated within the TW model.

Conclusions

Removal of space debris is a global issue that is becoming increasingly important. Methods of active de-orbiting defunct satellites are costly and technically demanding. Therefore, new approaches to efficient and effective cleanup of space debris are highly desirable. The nonlinear effect of high-power laser propagation in the atmosphere causes restrictions on ground-based laser systems for space debris cleaning. We have demonstrated that the thin window model provides high accuracy for light propagation and accurately predicts the phase distortion at the atmospheric edge. Thus it can be very efficient in multi-parametric optimization of ground systems. Initial phase distortion can compensate the deviations produced by self-focusing, and can almost completely remove the detrimental effects of self-focusing. A similar approach can be used to compensate for the detrimental effects of self-focusing in femtosecond material processing.

Appendix I

In this section we will discuss the accuracy of modeling using the TW model. We then check the accuracy of the model by comparison of the field in the center of the beam in the initial focal plane,

$$error(S) = \frac{|S_{NLSE} - S_{TW}|}{S_{NLSE}} \times 100\%,$$

the displacement of the focal spot,

$$error(F) = \frac{|F_{NLSE} - F_{TW}|}{F_{NLSE}} \times 100\%,$$

and the intensity maximum,

$$error[I(0,F)] = \frac{|I(0,F)_{NLSE} - I(0,F)_{TW}|}{I(0,F)_{NLSE}} \times 100\%,$$

calculated with the exact NLSE and the TW model.

In Fig. 7 we present the error calculations for different beam powers. In Fig. 7(a, b) we present the results for P/P_{cr} = 1000 and 5000 as a function of z_1. We see that, as was discussed in the text, the error is minimal for z_1 ~ 30 km, justifying the choice of z_1 used in the main text. We see that before the filamentation starts, for modest values of b the accuracy is good. For high intensity, P/P_{cr} >5000, the accuracy decreases but is still reasonable even for a completely filamented beam.

Acknowledgments

This work was supported by Russian Science Foundation (Grant No.14-21-00110). Part of the work was performed under the auspices of the U.S. Department of Energy by Lawrence Livermore National Laboratory under contract DE-AC52-07NA27344.

References

[1] Phipps CR, Baker KL, Libby SB, Liedahl DA, Olivier SA, Pleasance LD, et al. Removing orbital debris with lasers. Advances in Space Research 2012; **49**: 1283-1300.
[2] Rubenchik AM, Fedoruk MP, Turitsyn SK. The effect of self-focusing on laser space-debris cleaning. Light: Science & Applications 2014; **3**: e159.
[3] Marburger JH. Self-focusing: Theory. Progress in Quantum Electronics 1975; **4**: 35-110.
[4] Rubenchik AM, Erlandson AC, Liedahl D. Laser system for space debris cleaning. AIP Conference Proceedings 2012; **1464**: 448-453
[5] Zakharov VE, Rubenchik AM. Instability of waveguides and solitons in nonlinear media. Sov Phys JETP 2012; **38**: 494–500
[6] Fibich G, Eisenmann S, Ilan B, Zigler A. Control of Multiple Filamentation in Air. Optics Letters 2004; **29**: 1772-1774.
[7] Boyd RW, Lukishova SG, Shen YR (eds) Self-focusing: Past and Present. Fundamentals and Prospects. New York: Springer, 2009.
[8] Kaplan AE External Self-Focusing of Light by a Nonlinear Layer. Radiophys., Quant. Electron. 1969; **12**: 692-696.
[9] Weaire D, Wherrett BS, Miller DAB and Smith SD Effect of low-power nonlinear refraction on laser-beam propagation in InSb. Optics Letters 1979; **4**: 331-333.
[10] Goodman JW. Introduction to Fourier Optics. McGraw Hill: New-York, 1968.
[11] Shen Y. Principles of Nonlinear Optics. New York: Wiley Interscience, 1984.
[12] Turitsyn SK, Mezentsev VK, Dubov M, Rubenchik AM, Fedoruk MP, Podivilov EV. Sub-critical regime of femtosecond inscription. Optics Express 2007; **15**: 14750-14764.

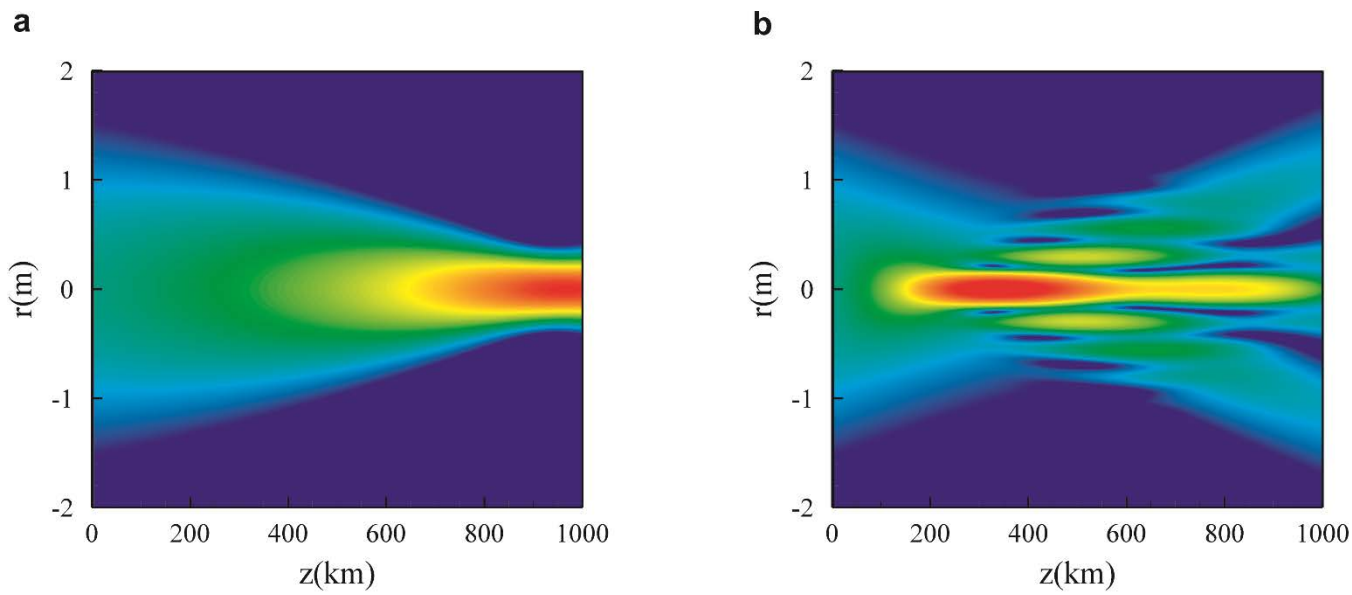

Figure 1. The normalized intensity distribution I(r, z)/I(0, 0) [with ($I(r,z) = |A(r,z)|^2$)].
(**a**) P_{in} / P_{cr} = 100, C = 5.93. (**b**) P_{in} / P_{cr} = 5000 (b), C = 5.93. These conditions correspond to a focusing distance L = 1000 km for the linear propagation.

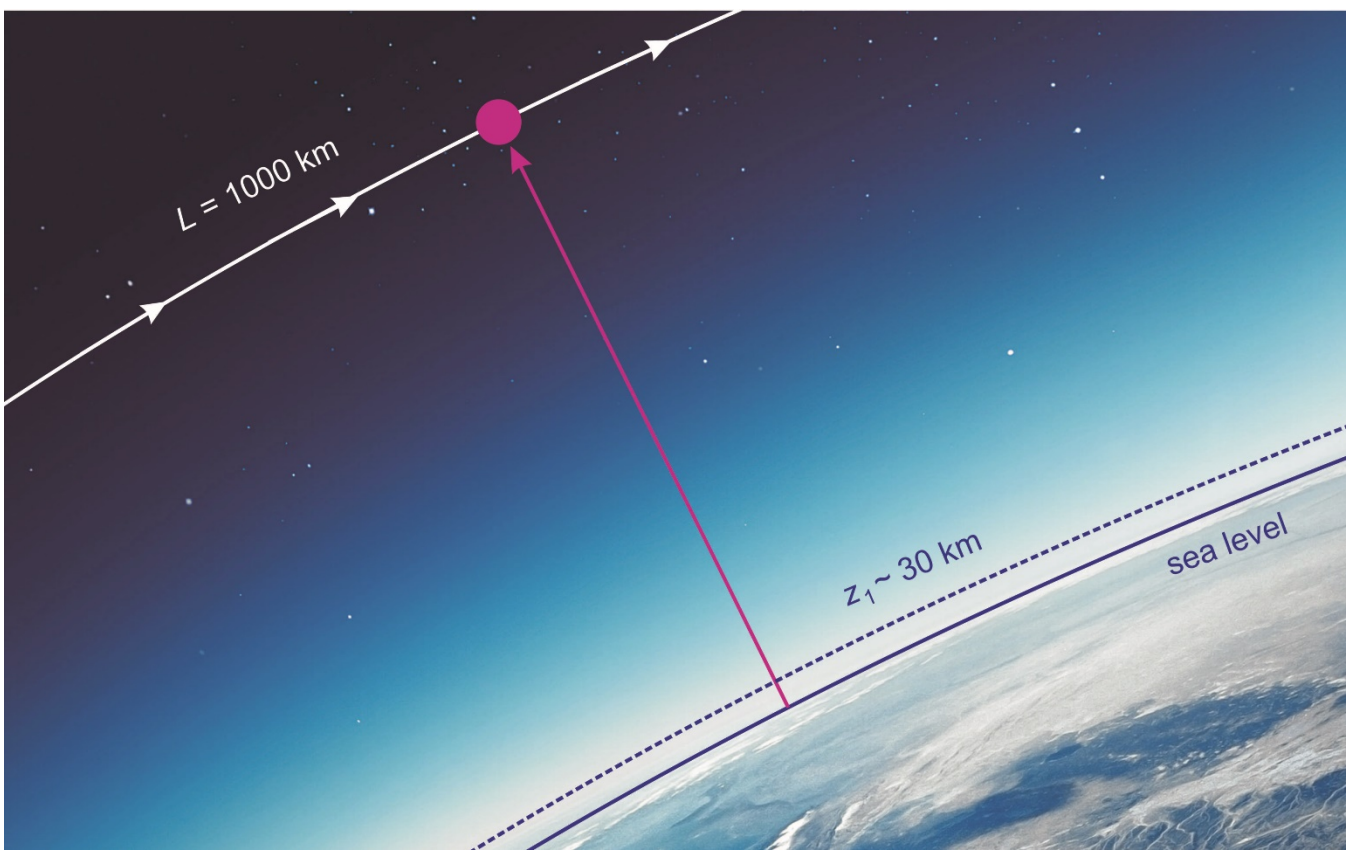

Figure 2. Illustration of the thin window model.

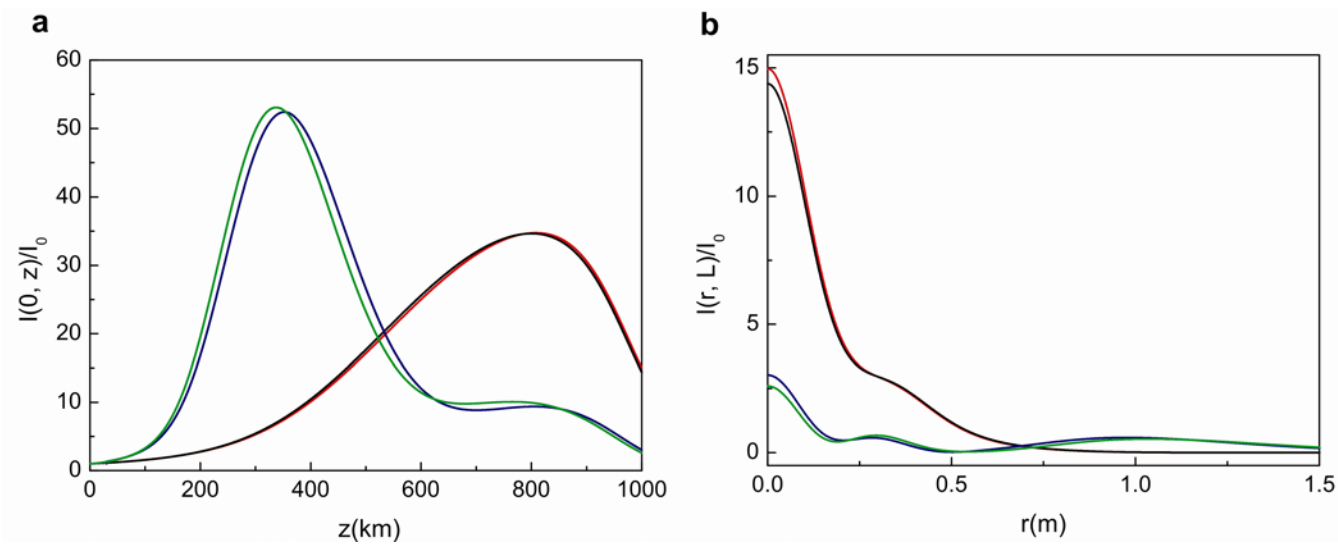

Figure 3. Comparison of the solution of the NLSE (1) with the TW model (3) for z_1 = 30 km.
(**a**) The peak intensity distribution along *z*.
(**b**) The radial intensity profile at the initial focal point *L* = 1000 km.
Black line: NLSE, P_{in} / P_{cr} = 1500. Red line: TW, P_{in} / P_{cr} = 1500.
Green line: NLSE, P_{in} / P_{cr} = 5000. Blue line: TW, P_{in} / P_{cr} = 5000.

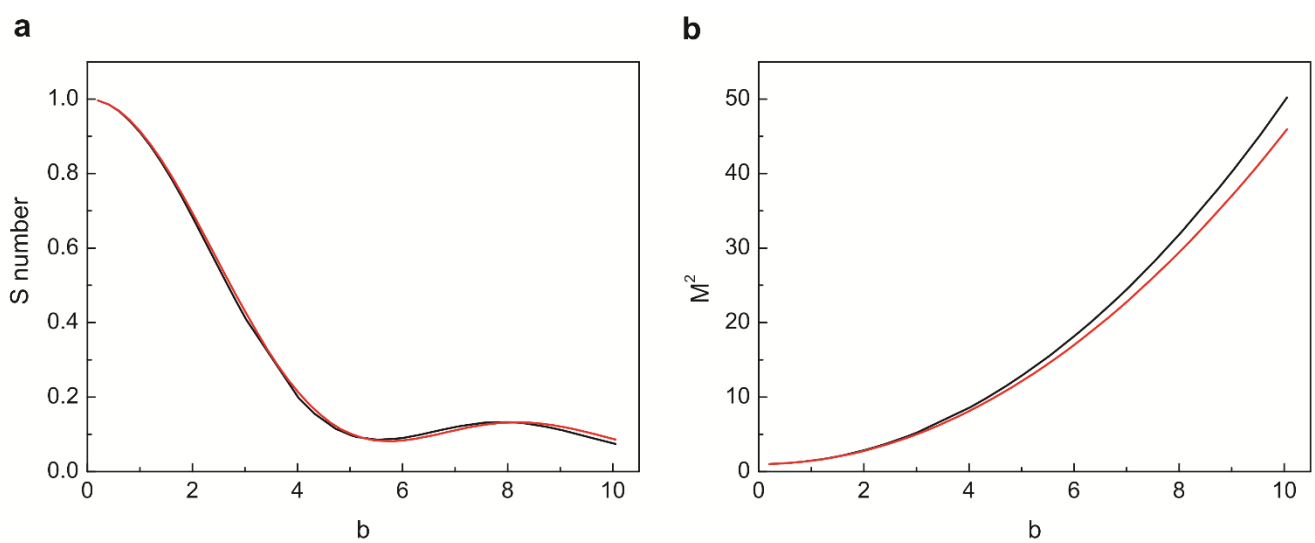

Figure 4. (**a**) Comparison of Strehl ratio computed from the TW model (9a) and the NLSE (1).
(**b**) Comparison of the beam quality parameter M^2 from formula (11) with results of direct modeling using the NLSE. Black line: NLSE. Red line: TW for z_1 = 30 km.

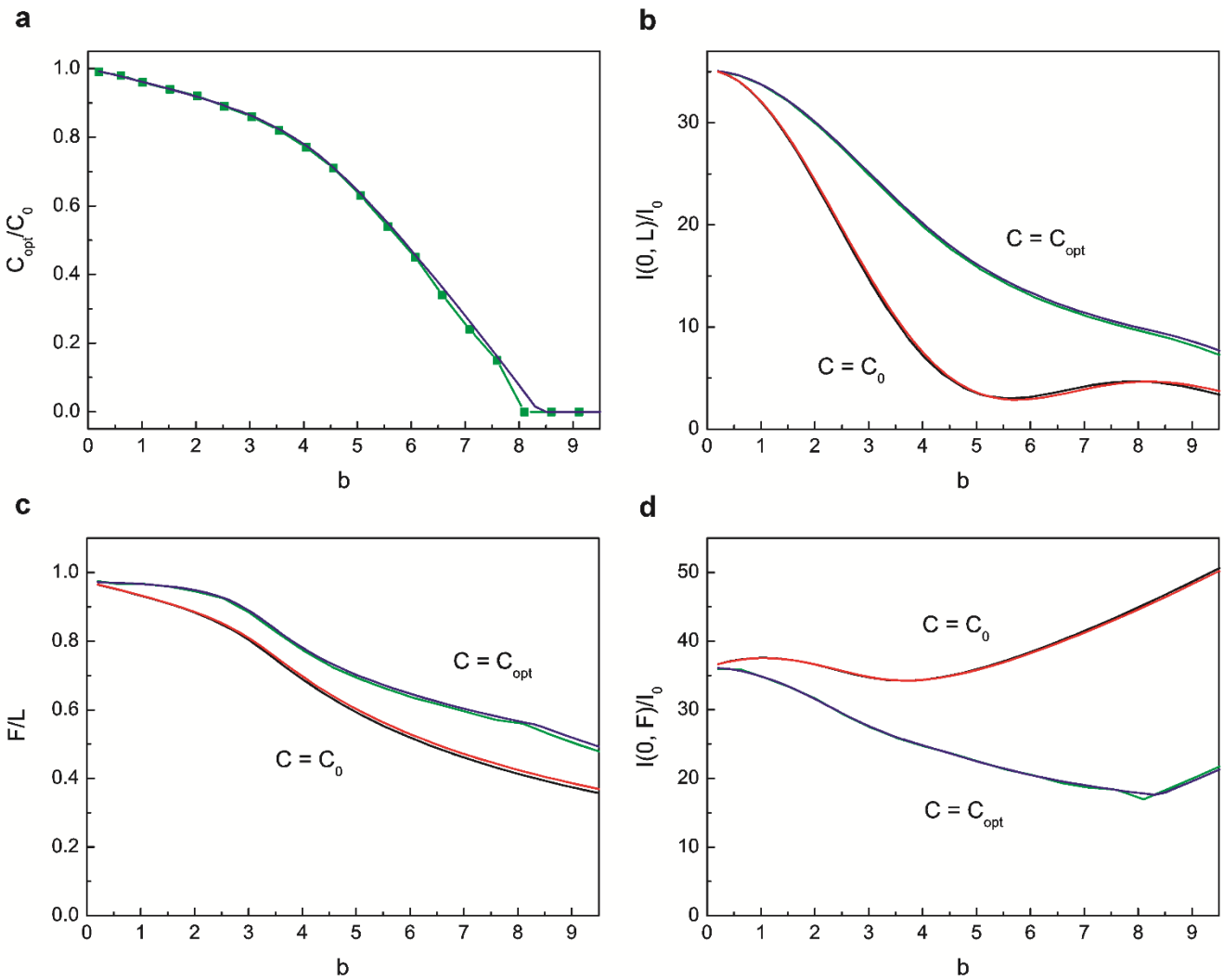

Figure 5. (**a**) The optimal chirp C_{opt} normalized by the initial chirp C as a function of b.
(**b**) The normalized intensity at the initial focal point L = 1000 km depending on b for the initial and optimal chirps.
(**c**) New focusing length F/L depending on b for the initial and optimal chirps.
(**d**) The normalized intensity at new focal points $I(0, F) = \max[I(r,z)]$ depending on b for the initial and optimal chirps. The maximum value of b corresponds to $P_{in} / P_{cr} = 5000$.

Black line: NLSE, C . Red line: TW, C .
Green line: NLSE, C_{opt}. Blue line: TW, C_{opt}.

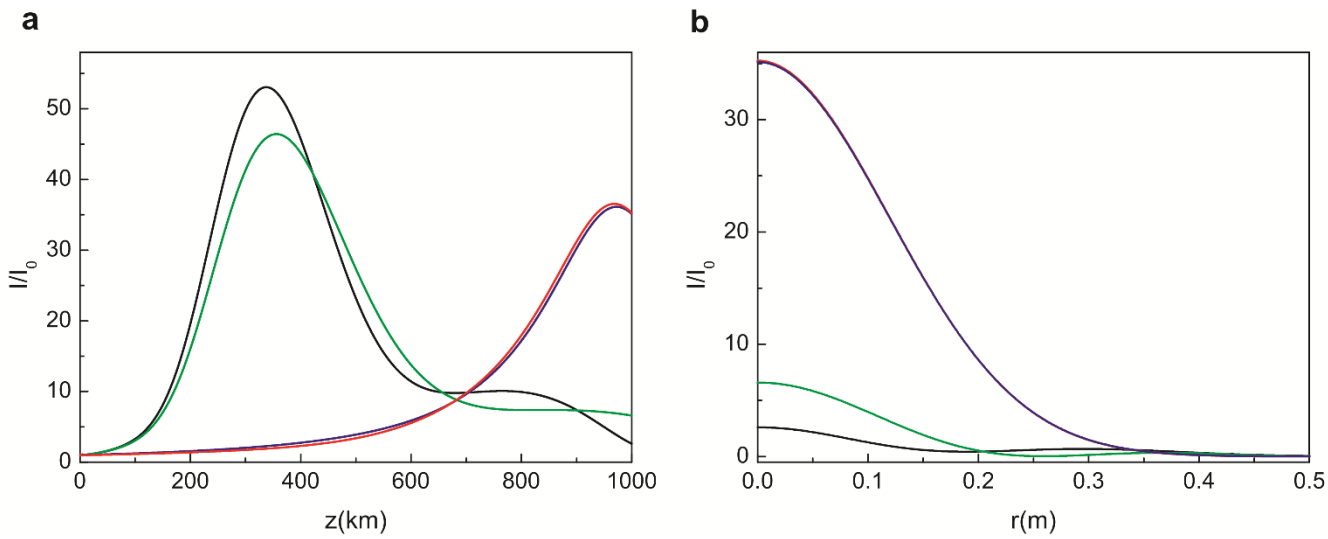

Figure 6 (**a**) Intensity distribution along z. (**b**) Radial distribution at the initial focal point L = 1000 km. P_{in} / P_{cr} = 5000. Black line: NLSE with $C = 5.93$ *corresponding to beam linear focusing at* $z = L$. Green line: NLSE with C = C_{opt}. Red line: NLSE with $C = 6.93$ and pre-imposed phase (13). Blue line: Propagation of Gaussian beam in the linear case. (Why blue line is not peaked at L=1000 (z1?)

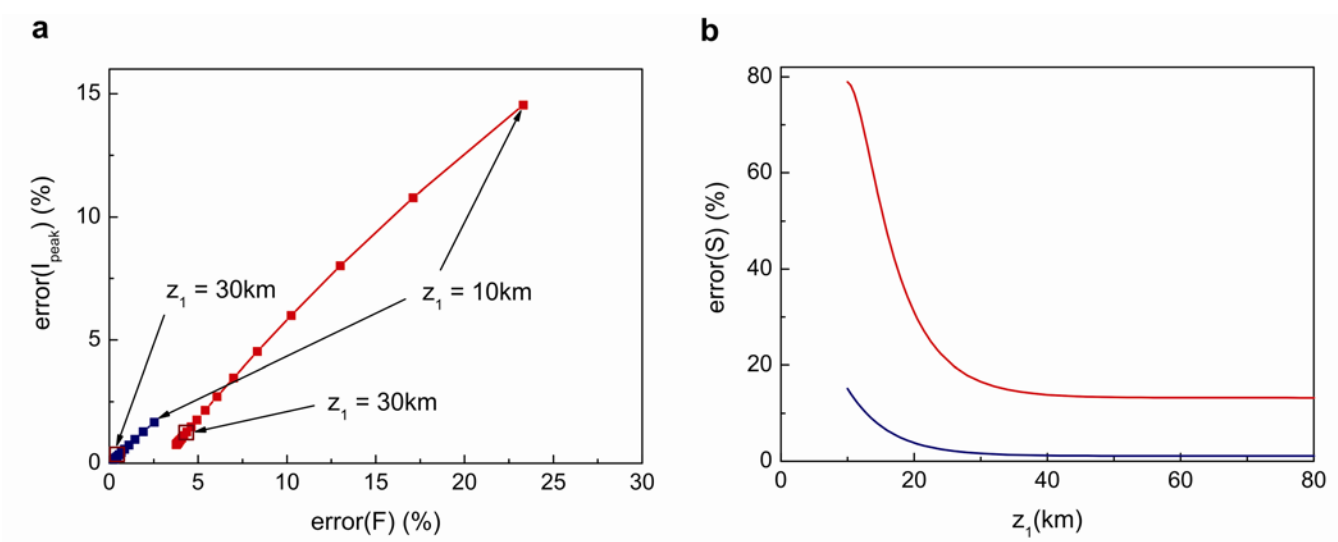

Figure 7 Determination of the optimal z_1. C = 5.93.
(**a**) error (F) and error [$I(0, F)$] depending on z_1. Plot points correspond to different values of z_1 from 10 to 80 km. From point to point z_1 varies with an increment step of 2 km.
(**b**) error(S) depending on z_1.
Blue line: P_{in} / P_{cr} = 1000. Red line: P_{in} / P_{cr} = 5000.